RSC Advances

ROYAL SOCIETY OF CHEMISTRY

www.rsc.org/advances

Exploring Metallic Phase of N_2O under High Pressure

Chunye Zhu,[1] Haixin Bi,[1] Shoutao Zhang,[1] Shubo Wei,[1] and Quan Li[2,1,*]

[1] *State Key Laboratory of Superhard Materials, Jilin University, Changchun 130012, China*

[2] *College of Materials Science and Engineering, Jilin University, Changchun 130012, China*

Table of contents entry

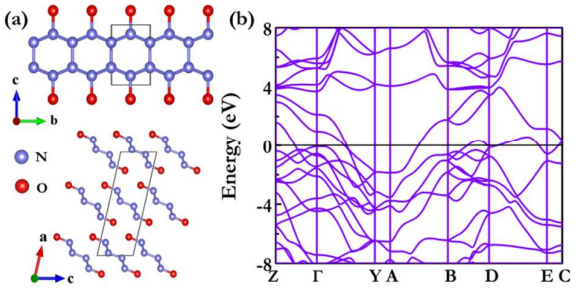

Using CALYPSO method, we proposed a new metallic structure of N_2O under high pressure.

ABSTRACT

Simple molecular solids are expected to undergo structural phase transitions to form framework or polymeric solids under high pressure. The high-pressure structures of N_2O have long attracted considerable attention. We combine the CALYPSO searching method with density functional theory to investigate the phase stabilities and structural changes of N_2O at high pressures. We find two metallic structures of N_2O which may be observed in high-pressure experiments. The current calculations reveal that the *C*2/*m* is the most stable structure over a pressure range of 177-194 GPa, and the other *C*2/*c* is metastable and only 10 meV/atom higher in energy than the *C*2/*m* structure at 180 GPa. At higher pressure, the metallic *C*2/*m* phase transforms into an insulating phase with space group of $P2_1/m$.

1. Introduction

Pressure is a thermodynamic parameter of paramount importance for chemical equilibria and chemical kinetics. Under high pressure, the interatomic distance become shorter and the bonding patterns of materials can be altered, causing profound effects on numerous physical and chemical properties.[1] High pressure plays an important role in the synthesis of new materials. Synthetic diamond is one of classic examples of high-pressure application.[2] Moreover, the pressure can also effectively lower the barrier of chemical reaction and can be used to synthesize compounds with distinct species, such as $NaCl_3$.[3]

Simple molecular solids are characterized by strong covalent intramolecular interaction and weak van der Waals intermolecular interaction. At high pressure, the distance between atoms becomes shorter, and the intermolecular interactions of molecular crystals become highly repulsive which increases the instability of electrons localized within intramolecular bonds. This leads to unexpected transformations which molecular solids get through a full reorganization of the chemical bond connectivity to reduce free energy such as ionization,[4-8] polymerization,[9-11] metallization[12, 13] and the like. The new classes of materials may exhibit entirely new electronic, optical, and physical properties.[14, 15] For example, pressure-induced polymerization of molecular crystals with super hardness,[16] superconductivity,[17] and high energy density[9, 18] have been found.

N_2O is one of the most extensively studied molecular crystals for its applications in medicine, refrigeration, and combustion reaction. The physical properties of N_2O and CO_2 are very similar, such as isoelectronic, linear molecules, and the nearly melting point. Although N_2O has no inversion symmetric since the O atom is located at one end, it has been shown that N_2O molecules solidify into a random head-to-tail orientation disorder at low pressures.[19, 20] N_2O is therefore expected to form similar structures with CO_2 at low pressures. In the solid state, the N_2O molecules crystallize into the same configurations as CO_2,[21] such as *Pa*-3[22] structure at ambient condition and *Cmca* structure above ~5 GPa.[19, 20, 23] Early experiments have found the solid N_2O

decomposes into an ionic crystal $NO^+NO_3^-$ and compressed N_2 molecules at high pressure and temprature.[6, 7] Recently, theoretical study of N_2O has predicted that N_2O forms a one-dimensional polymer with an all-nitrogen backbone analogous to *cis*-polyacetylene in which alternate N atoms are bonded to O atoms above 60 GPa.[24] Later on, the studied pressure range is up to 500 GPa,[25] a new N_2O nanotube structure is found to be the most stable form above 180 GPa. Generally，molecular solids will go through insulator-metal transition at sufficiently high pressures due to the broadening of electronic bands,[15, 26] e.g., solid O_2 transforms to metallic phase near 95 GPa[13] and iodine undergoes a pressure-induced insulator-metal transition near 16 GPa.[27] However, the metallic N_2O have not been found so far. With the evolution of computer simulation technology, useful theoretical research can be as an aid in the interpretation of experimental data and guide experiment.[28] Here, we perform our swarm structural searching method[29-31] combined with first-principles calculations to explore structures and physical properties of N_2O under high pressure.

2. Calculation methods

The structure searching was performed based on the particle swarm optimization algorithm as implemented in CALYPSO (Crystal structure AnaLYsis by Particle Swarm Optimization).[29-31] The method unbiased by any known structural information has been demonstrated by recent successes in predicting structures of various systems.[32-35] The underlying *ab-initio* structural relaxations and the electronic band structure calculations were performed within the framework of density functional theory (DFT) as implemented by the VASP (Vienna *Ab initio* Simulation Package) code.[36] The calculations were carried out at the generalized gradient approximation (GGA)[37] level using the Perdew-Burke-Ernzerh (PBE) of exchange correlation functional. The electronic wave functions were expanded in a plane-wave basis set with a cutoff energy of 1000 eV for all cases. The electron-ion interaction was described by means of projector augmented wave (PAW)[38] pseudopotential with $2s^22p^3$ and $2s^22p^4$ electrons as valence for N and O atoms, respectively. The Heyd-Scuseria-Ernzerhof (HSE)[39] hybrid functional is used to achieve an accurate

electronic band dispersion of stable phases. We employed the Bader charge analysis approach[40] for evaluating the charge transfer. Monkhorst-Pack k-point[41] meshes with a grid of 0.03 $Å^{-1}$ for Brillouin zone sampling were chosen to achieve the total energy convergence of less than 1 meV/atom. The phonon dispersion curves were computed by the direct supercell calculation method as implemented in the Phonopy program.[42]

3. Results and discussion

We have performed structure prediction simulations for N_2O with variable-cell simulation cell sizes of 1−4 and 6 formula units (f.u.) at 40-300 GPa. The enthalpy-pressure relations of various interesting structures are shown in Fig. 1. Analysis of our simulation results has confirmed the experimental *Cmca* structure and the earlier predicted 2-*d* polymer(*Pnma*-1),[25] *cis*-polymer (*Pnma*-2),[24] and nanotube structure ($P2_1$/m).[25] In addition, two exotic metallic structures: *C*2/*c* (8 f.u./cell) and *C*2/*m* (4 f.u./cell) were uncovered here. The *Cmca* structure transforms to the *cis*-polymer structure at about 57 GPa, in good agreement with previous calculations.[24] However, our results clarify and correct previous structural assignments at high pressures: the *C*2/*m* structure of N_2O becomes energetically preferable to *cis*-polymer structure above 177 GPa. Above 194 GPa, N_2O forms a nanotube $P2_1/m$ structure. We found that a *C*2/*c* structure is favored over the *cis*-polymer structure above 186 GPa. It should be note that *C*2/*c* structure is metastable phase and the enthalpy of *C*2/*c* structure is only 10 meV/atom higher in energy than that of *C*2/*m* structure at 180 GPa. Below we focus on these two new phases which may be synthesized at high pressure.

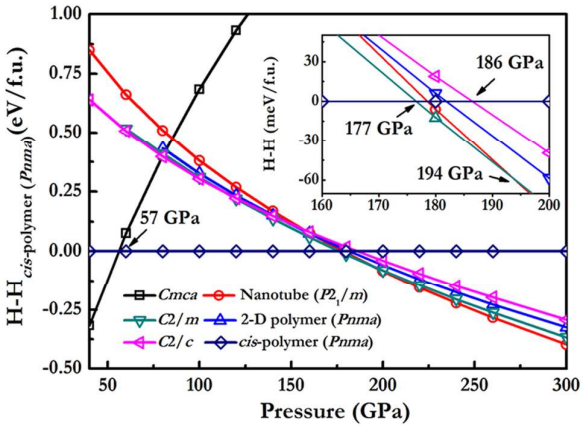

Fig. 1. The enthalpies per formula unit of various structures as a function of pressure with respect to *cis*-polymer structure of N_2O.

The crystal structures of *C*2/*c* and *C*2/*m* are shown in Fig.2, which are both layered structures. Layered structures also appear in the polymerized solids of other molecules, such as N_2,[43] CO,[44] and CO_2.[45] There are two types of N atom present in both *C2/c* and *C*2/*m* structure: one is N1 connected with both N atom and O atom, and the other is N2 only connected with N atom. At 180 GPa, from Fig. 2a, the layer of *C*2/*c* can be viewed as bulbs stacking. Every N atom is bonded with three neighbouring atoms, while each O atom is bonded with one N atom. The unit cell of the *C*2/*c* structure has 8 f.u. per cell with parameters of a = 4.954 Å, b = 3.668 Å, c = 7.819 Å and β = 125.333º, with O atoms at Wyckoff 8*f* position (-0.2084, -0.0016, 0.0766) and N atoms occupying two in equivalent 8*f* positions: (0.3384, -0.0036, 0.2172) and (0.3082, -0.1692, 0.8443). The *C*2/*m* structure possesses similar bonding states with that of the *C*2/*c* structure. The N atoms in the same layer form wrinkled N_6 rings. (Fig. 1c.). It is interesting that the *C*2/*m* structure of N_2O is related to the theoretically

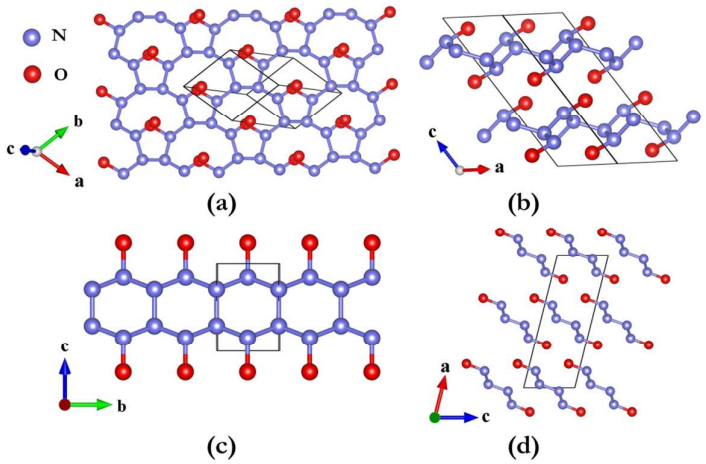

Fig. 2. The *C*2/*c* (up) and *C*2/*m* (down) structures at 200 GPa. (a) Top view of *C*2/*c* structure along the layered stacking direction. (b) Top view of *C*2/*c* structure along *b*-axis. (c) Top view of *C*2/*m* structure along the layered stacking direction. (d) Top view of *C*2/*m* structure along *b*-axis.

predicted *Cmcm* structure of solid CO,[44] which also contains six-membered C_6 rings. At 180 GPa, the optimized lattice parameters of *C*2/*m* are a = 8.556 Å, b = 2.183 Å, c = 3.188Å and β = 75.539º with O atoms at Wyckoff 4*i* position (0.1787, 0.5, 0.7631) and N atoms occupying two inequivalent 4*i* positions: (0.0258, 0, 0.2908) and (0.8755, 0.5, 0.8459). The interlayer distance decreases significantly with pressure while the intralayer structure is hardly affected.

To investigate the dynamical stabilities of our predicted N_2O structures, the phonon dispersions of *C*2/*c* and *C*2/*m* structures are shown in Fig. 3. No imaginary phonon frequencies are found in these two structures, indicating the dynamical stability. The cells of *C*2/*c* and *C*2/*m* contain 24 and 12 atoms, giving 72 and 36 phonon branches, respectively. The phonon bands of *C*2/*m* have very little dispersion along *Y*-*A* and *E*-*C* directions (which is the interlayer directions), showing that the corresponding interactions are weak.

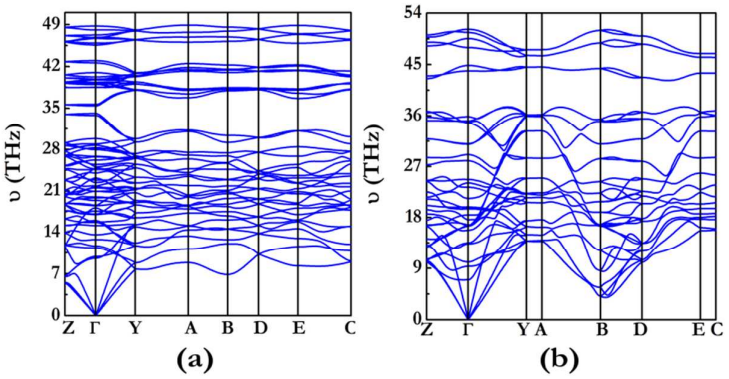

Fig. 3. Phonon dispersion relations of (a) *C*2/*c* at 200GPa, (b) *C*2/*m* at 180GPa.

The electronic band structure of *C*2/*c* and *C*2/*m* at 180 GPa are shown in Fig. 4. Due to the PBE calculations severely underestimate the band gaps, we also include band calculations using the HSE hybrid functional for comparison. Both PBE and HSE calculations reveal the metallic nature of *C*2/*c* and *C*2/*m* phases. For the *C*2/*m* phases, the dispersions of the electron bands are strong in the intralayers (e.g. along the *Γ*-*Y* direction), but very weak between the layers along the *Y*-*A* and *E*-*C* directions. This observation indicates that in-layer interactions are much stronger than the inter-layer direction.

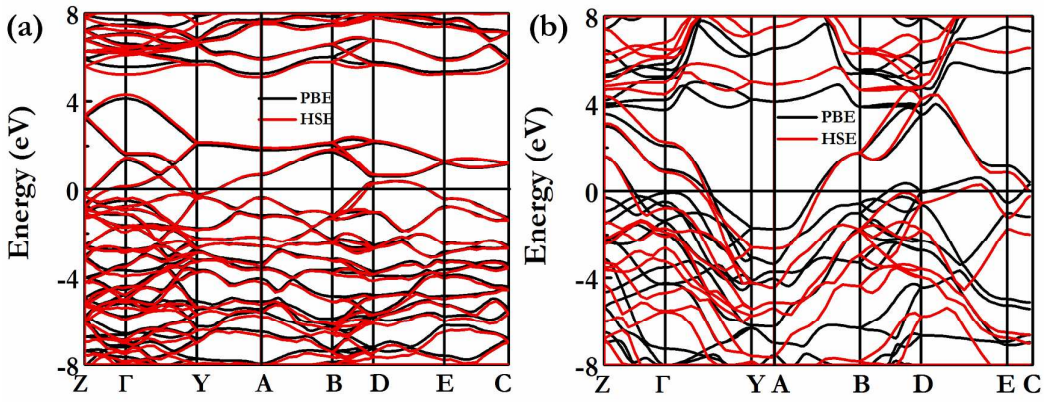

FIG. 4. Electronic band structures at 180 GPa for (a) *C*2/*c* and (b) *C*2/*m*

Chemical bonding behavior is the key to get a full understanding of the metallic nature of these structures. The nature of their bonding was probed by calculating the electron localization functions (ELF)[46] of Fig. 5. The ELF is a measure of relative electron localization, and large ELF values indicate there is a high tendency of electron pairing, such as cores, bonds, and lone pairs. The high electron localization can be seen in the region between adjacent N-N and N-O bonds in *C*2/*c* and *C*2/*m*, indicative of covalent bonding. Fig. 6 shows the bond lengths of *C*2/*c* and *C*2/*m* as a function of pressure. For the *C*2/*m* structure, the bond lengths of N1-N2 are remarkably larger than N2-N2 bond lengths. At 180 GPa, the bond length between two N2 atoms is 1.292 Å, prominently shorter than the N1-N2 bond length of 1.383 Å. By comparison with the N=N double bond in the HN_3 molecule (1.23 Å) [47], the N2-N2 bond can be reasonably classified as the double bond and the N1-N2 bond as the single bond. We employed the Bader charge analysis approach for evaluating the actual charge transfer between N and O atoms. The calculated O Bader charges are 6.45 *e*. The Bader charges indicate a substantial charge transfer from N to O, illustrating the mixture of ionic and covalent bonds appear between the N and O atoms. Each O atom forms a single N-O bond and accepts one electron from N1 atom to satisfy the octet rule. N1 atom loses one electron and forms three single bonds, and N2 atom forms two single bonds and one double bond. In consequence, every N has one remaining electron forming a set of π bonds spanning all N atoms in the same layer. The delocalized π electrons can be free to move throughout the same layer, and give rise to property of conductivity, which is similar to graphite. For the *C*2/*c* structure, the bond lengths of N1-N2 are nearly close to N2-N2 bond lengths. From Fig. 6a, the N1-N2 bond length dramatically decreases with the increasing pressure. At 260 GPa, N1-N2 bond length become shorter than the N2-N2 bond lengths. That is because the direction of N2-N2 bond is nearly parallel to the layers, while the direction of N1-N2 bond is along the layers stacking direction (Fig. 2b). The weak interaction of the inter-layer direction leads to the easier compression of N1-N2 bond. For *C*2/*c* structure at 180 GPa, the N-O bonding behavior is similar to that in *C*2/*m* structure. The calculated N2-N2 bond length is 1.309 Å and there are two types of

N1-N2 bond with alternate distances of 1.321 Å and 1.323 Å. The valence bond description suggests alternating single and double bonds. This bonding pattern also forms the delocalized π electrons which is responsible of metallic nature of C2/c structure. At 194 GPa, the *C*2/*m* structure transforms into the $P2_1$/m structure.[25] The $P2_1$/m structure is proposed by the earlier theoretical prediction. In this structure, O atom bonded with two N atoms, and every N atom has a lone pair with two single N-N bonds and one single N-O bond. The covalent bonds and lone-pair electrons are together the driving force for the insulating character of $P2_1/m$ structure, since the electrons are highly localized. The metal-insulator transition is previously exemplified in dense lithium,[48] sodium,[49] and oxygen.[50, 51] In contrast to oxygen, the metal-insulator transition pressure (1.9 TPa) is considerably higher than 194 GPa in the current N_2O.

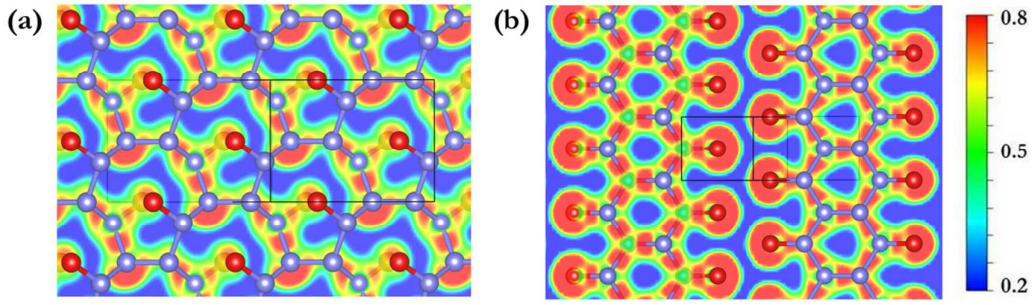

FIG. 5.Calculated electron localization functions (ELF) for (a) *C*2/*c* at 180 GPa, and (b) *C*2/*m* at 180 GPa

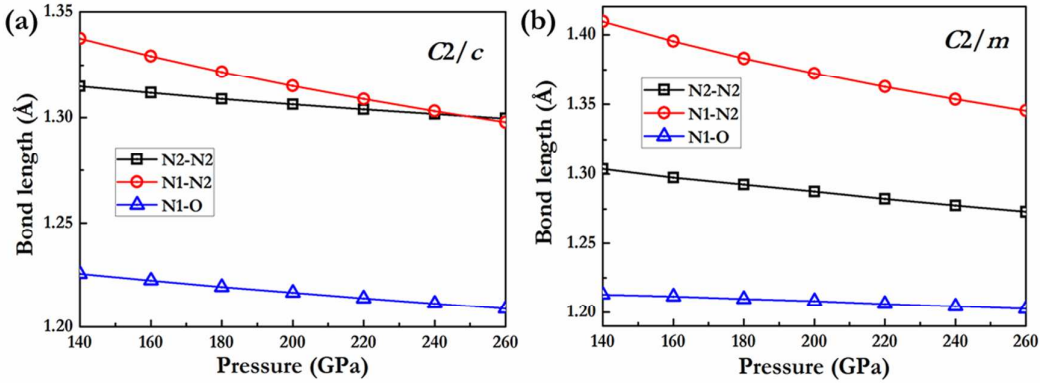

FIG. 6. Calculated bond lengths as a function of pressure. (a) *C*2/*c* and (b) *C*2/*m*

4. Conclusions

Using the CALYPSO method for crystal structure prediction combined with first-principle calculations, two novel metallic structures of N_2O with space group *C*2/*m* and *C*2/*c* were discovered. The *C*2/*m* structure becomes the most stable phase above 177 GPa and it transforms into an insulate $P2_1/m$ structure above 194 GPa. Two metallic structures are both layered structures, and every N atom is threefold-coordinated, while each O atom is only bonded with one N atom. The metallic behavior of N_2O is derived from delocalized π electrons. The N_2O structures can be tuned with increasing pressure from insulating behavior (*Pnma* phases), to melallic (*C*2/*m*) and then back to insulating ($P2_1/m$). The predicted formation of metallic structure in N_2O represents a significant step forward in understanding the behavior of N_2O and other molecular crystals at high pressures.

Acknowledgements

This work was supported by the China 973 Program(2011CB808200), the Natural Science Foundation of China underNo.51202084, 11474125, and 11274136, the2012 Changjiang Scholars Program of China, Changjiang Scholarand Innovative Research Team in University (IRT1132). Parts of the calculations were performed in the High Performance Computing Center (HPCC) of Jilin University.

Corresponding Author*

(Q. Li) Tel: +86-431-85167557. E-mail: liquan777@jlu.edu.cn.

References

1 W. Grochala, R. Hoffmann, J. Feng, N. W. Ashcroft, *Angew. Chem. Int. Ed.*, 2007, **46**, 3620.

2 F. Bund, *J. Chem. Phys.*, 1963, **38**, 631.

3 W. Zhang, A. R. Oganov, A. F. Goncharov, Q. Zhu, S. E. Boulfelfel, A. O. Lyakhov, E. Stavrou, M. Somayazulu, V. B. Prakapenka and Z. Konopkova, *Science*, 2013, **342**, 1502.

4 Y. Wang, H. Liu, J. Lv, L. Zhu, H. Wang and Y. Ma, *Nat.Commun.*, 2011, **2**, 563.

5 C. J. Pickard and R. Needs, *Nature. Mater.*, 2008, **7**, 775.

6 M. Somayazulu, A. Madduri, A. F. Goncharov, O. Tschauner, P. F. McMillan, H.-k. Mao and R. J. Hemley, *Phys. Rev. Lett.*, 2001, **87**, 135504.

7 C. S. Yoo , V. Iota , H. Cynn , M. Nicol , J. H. Park , T. Le Bihan , and M. Mezouar, *J. Phys. Chem. B*., 2003, **107**, 5922.

8 A. Yu. Kuznetsov, L. Dubrovinsky, A. Kurnosov, M. M. Lucchese, W. Crichton, and C. A. Achete1, *Adv Phys Chem.*, 2009, doi: 10.1155/2009/180784.

9 M. J. Lipp, W. J. Evans, B. J. Baer and C.-S. Yoo, *Nature. Mater.*, 2005, **4**, 211-215.

10 M. I. Eremets, A. G. Gavriliuk, I. A. Trojan, D. A. Dzivenko and R. Boehler, *Nature. Mater.*, 2004, **3**, 558.

11 V. Iota, C. Yoo and H. Cynn, *Science*, 1999, **283**, 1510.

12 Y. Fujii, K. Hase, N. Hamaya, Y. Ohishi, A. Onodera, O. Shimomura and K. Takemura, *Phys. Rev. Lett.*, 1987, **58**, 796.

13 Y. Akahama, H. Kawamura, D. Häusermann, M. Hanfland and O. Shimomura, *Phys. Rev. Lett.*, 1995, **74**, 4690.

14 V. Schettino and R. Bini, *Phys. Chem. Chem. Phys.*, 2003, **5**, 1951.

15 R. J. Hemley, *Annu. Rev. Phys. Chem.*, 2000, **51**, 763.

16 C. Yoo, H. Cynn, F. Gygi, G. Galli, V. Iota, M. Nicol, S. Carlson, D. Häusermann and C. Mailhiot, *Phys. Rev. Lett.*, 1999, **83**, 5527.

17 N. Ashcroft, *Phys. Rev. Lett.*, 2004, **92**, 187002.

18 C. Mailhiot, L. Yang and A. McMahan, *Phys. Rev. B.*, 1992, **46**, 14419.

19 R. Mills, B. Olinger, D. Cromer and R. Lesar, *J. Chem. Phys.*, 1991, **95**, 5392.

20 B. Kuchta, R. Etters and R. LeSar, *J. Chem. Phys.*, 1992, **97**, 5662.

21 K. Aoki, H. Yamawaki, M. Sakashita, Y. Gotoh and K. Takemura, *Science*, 1994, **263**, 356.

22 W. C. Hamilton and M. Petrie, *J. Phys. Chem.*, 1961, **65**, 1453.

23 V. Iota, J. Park and C. Yoo, *Phys. Rev. B.*, 2004, **69**, 064106.

24 H. Xiao, Q. An, W. A. Goddard, W.-G. Liu and S. V. Zybin, *Proc. Nati. Acad. Sci.*, 2013, **110**, 321.

25 Q. An, H. Xiao, W. A. Goddard III and X. Meng, *J. Phys. Chem. Letts.*, 2014, **5**, 485.

26 C.-S. Yoo, *Phys. Chem. Chem. Phys.*, 2013, **15**, 7949.

27 A. Balchan and H. Drickamer, *J. Chem. Phys.*, 1961, **34**, 1948.

28 E. Zurek and W. Grochala, *Phys. Chem. Chem. Phys.*, 2015, **17**, 2917.

29 Y. Wang, J. Lv, L. Zhu and Y. Ma, *Phys. Rev. B.*, 2010, **82**, 094116.

30 Y. Wang, J. Lv, L. Zhu and Y. Ma, *Comput. Phys. Commun.*, 2012, **183**, 2063.

31 Y. Wang, M. Miao, J. Lv, L. Zhu, K. Yin, H. Liu and Y. Ma, *J. Chem. Phys.*, 2012, **137**, 224108.

32 L. Zhu, H. Liu, C. J. Pickard, G. Zou and Y. Ma, *Nature. Chem.*, 2014, **6**, 644.

33 S. Lu, Y. Wang, H. Liu, M.-s. Miao and Y. Ma, *Nat.Commun.*, 2014, **5**, 3666.

34 Q. Li, D. Zhou, W. Zheng, Y. Ma and C. Chen, *Phys. Rev. Lett.*, 2013, **110**, 136403.

35 M. Zhang, H. Liu, Q. Li, B. Gao, Y. Wang, H. Li, C. Chen and Y. Ma, *Phys. Rev. Lett.*, 2015, **114**, 015502.

36 G. Kresse and J. Furthmüller, *Phys. Rev. B.*, 1996, **54**, 11169.

37 J. P. Perdew, K. Burke and M. Ernzerhof, *Phys. Rev. Lett.*, 1996, **77**, 3865.

38 G. Kresse and D. Joubert, *Phys. Rev. B.*, 1999, **59**, 1758.

39 J. Heyd, G. E. Scuseria and M. Ernzerhof, *J. Chem. Phys.*, 2003, **118**, 8207.

40 W. Tang, E. Sanville and G. Henkelman, *J. Phys.: Condens.Matter*, 2009, **21**, 084204.

41 H. J. Monkhorst and J. D. Pack, *Phys. Rev. B.*, 1976, **13**, 5188.

42 A. Togo, F. Oba and I. Tanaka, *Phys. Rev. B.*, 2008, **78**, 134106.

43 J. Sun, D. D. Klug, R. Martoňák, J. A. Montoya, M.-S. Lee, S. Scandolo and E. Tosatti, *Proc.Nati. Acad.Sci.*, 2009, **106**, 6077.

44 J. Sun, D. D. Klug, C. J. Pickard and R. J. Needs, *Phys. Rev. Lett.*, 2011, **106**, 145502.

45 Y. Ma, A. R. Oganov, Z. Li, Y. Xie and J. Kotakoski, *Phys. Rev. Lett.*, 2009, **102**, 065501.

46 A. D. Becke and K. E. Edgecombe, *J. Chem. Phys.* 1990, **92**, 5397.

47 J. Evers, M. Gobel, B. Krumm, F. Martin, S. Medvedyev, G. Oehlinger, F. X. Steemann, I. Troyan, T. M. Klapotke and M. I. Eremets, *J. Am. Chem. Soc*., 2011, **133**, 12100

48 J. Neaton and N. Ashcroft, *Nature*, 1999, **400**, 141.

49 Y. Ma, M. Eremets, A. R. Oganov, Y. Xie, I. Trojan, S. Medvedev, A. O. Lyakhov, M. Valle and V. Prakapenka, *Nature*, 2009, **458**, 182.

50 L. Zhu, Z. Wang, Y. Wang, G. Zou, H.-k. Mao and Y. Ma, *Proc.Nati. Acad.Sci.*, 2012, **109**, 751.

51 J. Sun, M. Martinez-Canales, D. D. Klug, C. J. Pickard and R. J. Needs, *Phys. Rev. Lett.*, 2012, **108**, 045503.